J|A|C|S
ARTICLES
Published on Web 04/10/2002

A Density Functional Theory Study Clarifying the Reactions of Conjugated Ketenes with Formaldimine. A Plethora of Pericyclic and Pseudopericyclic Pathways

Chun Zhou and David M. Birney*

Contribution from the Department of Chemistry and Biochemistry, Texas Tech University, Lubbock, Texas 79409-1061

Received November 16, 2001

Abstract: The reactions of vinylketene (**1a**), imidoylketene (**1b**), and formylketene (**1c**) with formaldimine (**2**) were studied at the B3LYP/6-31G* level. For the cycloadditions of these conjugated ketenes with **2**, several possible pathways to both [4 + 2] and [2 + 2] products were examined. The lowest energy [2 + 2] pathways are, in most cases, calculated to be stepwise, forming the products via rate-determining conrotatory electrocyclization of zwitterionic intermediates. However, concerted transition structures analogous to the ketene plus ethene [2 + 2] cycloaddition reaction were also located; the existence of multiple transition states offers a resolution to a long-standing controversy regarding the mechanism of ketene plus imine cycloadditions. Both stepwise and concerted [4 + 2] pathways were calculated for **2b** and for **2c**; both these pathways are pseudopericyclic. The inherently low barriers associated with pseudopericyclic transition states provide an explanation of the experimental preference for [4 + 2] cycloadditions of α-oxoketenes and predict [4 + 2] cycloadditions should also be favored for imidoylketenes. For a vinylketene constrained to a *Z*-geometry, the concerted [4 + 2] cycloaddition is also predicted to be the lowest energy pathway. An explanation is offered for the unusual thermal equilibration from a six-membered ring (**3d**) to a four-membered ring (**4d**) observed by Sato et al. Transition structures for facile pseudopericyclic 1,3- and 1,5-hydrogen shifts in the zwitterions were also calculated.

Introduction

Ketenes have been extensively studied since Staudinger's original discovery in 1905,[1] and their structures, reactivities, and utility in organic synthesis are well documented.[2] The distinctive [2 + 2] cycloadditions of ketenes have been of particular utility in synthetic methodology; for example, the cycloaddition with alkenes provides an efficient synthesis of cyclobutenones, [2c] while the cycloaddition with imines (the Staudinger reaction[3]) provides a concise route to β-lactam antibiotics.[4] There has been significant interest in and controversy over the mechanism of this latter cycloaddition for many years, with extensive experimental[5] and computational studies.[5e,g,6] The common cis-stereochemistry of the reactions of ketenes with alkenes has generally been rationalized in terms of a concerted, orthogonal transition state, as in Figure 1A.[2c,7] This structure is similar to that proposed by Woodward and Hoffmann,[8] although their original description of it as a [π2s + π2a] cycloaddition has since been revised. Early MCSCF/4-31G (four-electron, four-orbital) calculations by Bernardi and Robb suggested a two-step biradical mechanism;[9] however, there does not seem to be independent support for this mechanistic possibility. Calculations by Houk and Wang also indicated an orthogonal and highly asynchronous transition state.[10] This was interpreted as indicating a carbene-like mechanism in which the ethylene π-bond adds as a nucleophile to the in-plane LUMO of the ketene, and only past the transition state is there substantial bonding to the β-carbon. MP2 calculations by Yamabe et al. were discussed in terms of two separate one-centered FMO interactions.[11] Wong and Ma have recently reported a thorough computational study

* To whom correspondence should be addressed. E-mail: david.birney@ttu.edu.

(1) Staudinger, H. *Chem. Ber.* **1905**, *38*, 1735−1739.
(2) (a) Ulrich, H. Cycloaddition Reactions of Heterocumulenes. In *Organic Chemistry*; Blomquist, A. T., Ed.; Academic Press: New York, 1967; Vol. 9, pp 38−109. (b) Hyatt, J. A.; Raynolds, P. W. In *Organic Reactions*; Paquette, L. A., Ed.; John Wiley & Sons: New York, 1994; Vol. 45, pp 159−636. (c) Tidwell, T. T. *Ketenes*; John Wiley & Sons: New York, 1995.
(3) Staudinger, H. *Liebigs Ann. Chem.* **1907**, *365*, 51.
(4) (a) Georg, G. I. *The Organic Chemistry of β-Lactams*; VCH: New York, 1992. (b) Page, M. I. *The Chemistry of β-Lactams*; Blackie Academic and Professional: New York, 1996.
(5) (a) Brady, W. T.; Shieh, C. H. *J. Org. Chem.* **1983**, *48*, 2499−2502. (b) Brady, W. T.; Gu, Y. Q. *J. Org. Chem.* **1989**, *54*, 2838−2842. (c) Lynch, J. E.; Riseman, S. M.; Laswell, W. L.; Tschaen, D. M.; P. Volante, R.; Smith, G. B.; Shinkai, I. *J. Org. Chem.* **1989**, *54*, 3792−3796. (d) Pacansky, J.; Chang, J. S.; Brown, D. W.; Schwarz, W. *J. Org. Chem.* **1982**, *47*, 2233−2234. (e) Palomo, C.; Cossío, F. P.; Odiozola, J. M.; Oiarbide, M.; Ontoria, J. M. *J. Org. Chem.* **1991**, *56*, 4418−4428. (f) Araki, K.; Wichtowski, J. A.; Welch, J. T. *Tetrahedron Lett.* **1991**, *32*, 5461−5464. (g) Palomo, C.; Cossío, F. P.; Cuevas, C.; Lecea, B.; Mielgo, A.; Romãn, P.; Luque, A.; Martinez-Ripoll, M. *J. Am. Chem. Soc.* **1992**, *114*, 9360−9369. (h) Welch, J. T.; Araki, K.; Kawecki, R.; Wichtowski, J. A. *J. Org. Chem.* **1993**, *53*, 2454−2462. (i) Birchler, A. G.; Liu, F.; Liebeskind, L. S. *J. Org. Chem.* **1994**, *59*, 7737−7745. (j) Palomo, C.; Aizpurua, J. M.; Legido, M.; Galarza, R.; Deya, P. M.; Dunogues, J.; Picard, J. P.; Ricci, A.; Seconi, G. *Angew. Chem., Int. Ed. Engl.* **1996**, *35*, 1239−1241. (k) Podlech, J.; Linder, M. R. *J. Org. Chem.* **1997**, *62*, 5873−5883. (l) Palomo, C.; Ganboa, I.; Kot, A.; Dembkowski, L. *J. Org. Chem.* **1998**, *63*, 6398−6400. (m) Hafez, A. M.; Taggi, A. E.; Wack, H.; Drury, W. J., III; Lectka, T. *Org. Lett.* **2000**, *2*, 3963−3965. (n) Emtenäs, H.; Soto, G.; Hultgren, S. J.; Marshall, G. R.; Almqvist, F. *Org. Lett.* **2000**, *2*, 2065−2067. (o) Emtenäs, H.; Alderin, L.; Almqvist, F. *J. Org. Chem.* **2001**, *66*, 6756−6761.

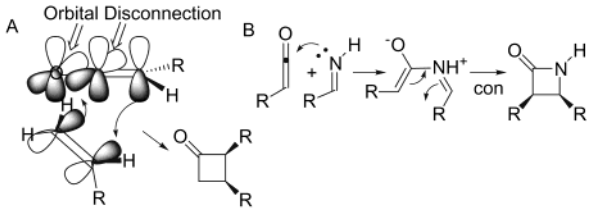

Figure 1. (A) Orbital interactions in the concerted cycloaddition of ketene with ethylene. (B) Stepwise mechanism for the [2 + 2] cycloaddition of ketenes with imines. Both mechanisms predict stereoselective formation of the cis-disubstituted products.

of ketene and its reaction with ethylene at the G2 level.[12] This again gives a similar geometry for the concerted [2 + 2] cycloaddition, and the calculated barriers are comparable to those determined experimentally.

In contrast to the concerted reaction with ethylene, there is substantial evidence, both experimental[5] and computational,[5e,g,6a−e,g,h,j,k,m−o] that the Staudinger reaction of a ketene with an imine proceeds via a zwitterionic (dipolar) intermediate as shown in Figure 1B. Thus, nucleophilic attack of the imine on the in-plane LUMO of the ketene gives the intermediate, which cyclizes via a four-electron, conrotatory electrocyclization to give the β-lactam. These electrocyclizations[5g,6c,d,j,k,m,n,13] often show significant torquoselectivity.[14] This mechanism also explains the observed cis-stereochemistry of the products; the more stable (*E*)-imine attacks the ketene anti to the large group, and subsequent conrotarory electrocyclization gives the cis product, as shown in Figure 1B.

Curiously, no one seems to have recognized the possibility of a concerted transition state similar to the reaction of ketene with ethylene. A higher energy transition state has been reported by Xu, Fang, and Fu;[6f,i] IRC calculations indicated it was not connected to any zwitterions. Subsequently, Sordo et al. reported a similar higher energy transition structure at the RHF/6-31G* level and described it as disrotatory.[6k] However, this description seems unreasonable as orbital symmetry forbidden reactions[8] are usually poorly described by single configuration wave functions as at the RHF level.[15] Our results below suggest that these structures are better understood as having orbital topology equivalent to the ketene plus ethylene transition state (Figure 1A).

Recently, there have been numerous reports of [4 + 2] cycloadditions in which a ketene is the dienophile. Yamabe et al. have provided NMR evidence for [4 + 2] cycloadditions involving the carbonyl of the ketene with dienes.[16] The observation of [4 + 2] products from the reaction of ketenes with α,β-unsaturated imines has been taken to provide support for the importance of the zwitterionic intermediate.[5a,6o,17,18] In these cases, the intermediates could close either by a four-centered or six-centered electrocyclization to give the [2 + 2] or [4 + 2] products, respectively.

Reactions of conjugated ketenes such as vinylketene (**1a**), imidoylketene (**1b**), and formylketene (**1c**) have been of both experimental and theoretical interest to our group[19] and to others.[2c,20] In principle, these ketenes can undergo both [2 + 2] and [4 + 2] cycloadditions, in the latter case participating as the diene. Barbaro et al. reported that vinylmethylketene reacted with *N*-phenylbenzaldehyde imine at room temperature and formed [2 + 2] cycloadducts (eq 1).[20a] Sharma et al. have studied reactions of various imines with butadienylketene and observed products from [2 + 2] cycloadditions as well.[20d,g] Similarly, [2 + 2] cycloaddition products are formed by vinylketenes with other electron-rich species such as enol ethers, alkynyl ethers, ynamines, or siloxyacetylenes.[20a,b] In contrast, vinylketenes undergo [4 + 2] cycloadditions with themselves,[20i] with enamines,[20j] dimethyl acetylenedicarboxylate, ethyl cyanoacrylate, nitroalkenes, cyanoallene, and, in the case of silylvinylketenes, with imines.[20e,f]

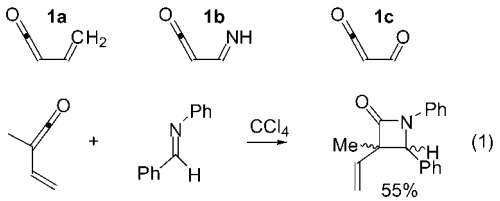

(1)

α-Oxoketenes such as **1c** undergo [4 + 2] cycloadditions with a wide range of substrates, including ketones, enol ethers, and

(6) (a) Sordo, J. A.; Gonzalez, J.; Sordo, T. L. *J. Am. Chem. Soc.* **1992**, *114*, 6249−6251. (b) Cossío, F. P.; Ugalde, J. M.; Lopez, X.; Lecea, B.; Palomo, C. *J. Am. Chem. Soc.* **1993**, *115*, 995−1004. (c) López, R.; Sordo, T. L.; Sordo, J. A.; González, J. *J. Org. Chem.* **1993**, *58*, 7036−7037. (d) Cossío, F. P.; Arrieta, A.; Lecea, B.; Ugalde, J. M. *J. Am. Chem. Soc.* **1994**, *116*, 2085−2093. (e) Arrastia, I.; Arrieta, A.; Ugalde, J. M.; Cossío, F. P. *Tetrahedron Lett.* **1994**, *35*, 7825−7828. (f) Xu, Z.-F.; Fang, D.-C.; Fu, X.-Y. *J. Mol. Struct. (THEOCHEM)* **1994**, *305*, 191−196. (g) Assfeld, X.; Ruiz-Lopez, M. F.; Gonzalez, J.; Lopez, R.; Sordo, J. A.; Sordo, T. L. *J. Comput. Chem.* **1994**, *15*, 597−487. (h) Assfeld, X.; Lopez, R.; Ruiz-Lopez, M. F.; Gonzalez, J.; Sordo, T. L.; Sordo, J. A. *J. Mol. Struct. (THEOCHEM)* **1995**, *331*, 1−2. (i) Fang, D.-C.; Fu, X.-Y. *J. Mol. Struct. (THEOCHEM)* **1995**, *331*, 3. (j) Lecea, B.; Arrastia, I.; Arrieta, A.; Roa, G.; Lopez, X.; Arriortua, M. I.; Ugalde, J. M.; Cossío, F. P. *J. Org. Chem.* **1996**, *61*, 3070−3079. (k) Lopez, R.; Ruiz-Lopez, M. F.; Rinaldi, D.; Sordo, J. A.; Sordo, T. L. *J. Phys. Chem.* **1996**, 10600−10608. (l) Fang, D.-C.; Fu, X.-Y. *Int. J. Quantum Chem.* **1996**, *57*, 1107−1114. (m) Arrieta, A.; Lecea, B.; Cossío, F. P. *J. Org. Chem.* **1998**, *63*, 5869−5876. (n) Arrieta, A.; Cossío, F. P.; Lecea, B. *J. Org. Chem.* **2000**, *65*, 8458−8464. (o) Bharatam, P. V.; Kumar, R. S.; Mahajan, M. P. *Org. Lett.* **2000**, *2*, 2725−2728. (p) Assfeld, X.; López, R.; Ruiz-López, M. F.; González, J.; Sordo, T. L.; Sordo, J. A. *J. Mol. Struct. (THEOCHEM)* **1995**, *1*, 331.
(7) Al-Husaini, A. H.; Muqtar, M.; Ali, S. A. *Tetrahedron* **1991**, *47*, 7719−7726.
(8) Woodward, R. B.; Hoffmann, R. *The Conservation of Orbital Symmetry*; Verlag Chemie, GmbH: Weinheim, 1970.
(9) (a) Bernardi, F.; Bottoni, A.; Robb, M. A.; Venturini, A. *J. Am. Chem. Soc.* **1990**, *112*, 2106−2114. (b) Reguero, M.; Pappalardo, R. R.; Robb, M. A.; Rzepa, H. S. *J. Chem. Soc., Perkin Trans. 2* **1993**, 1499−1502.
(10) Wang, Z.; Houk, K. N. *J. Am. Chem. Soc.* **1990**, *112*, 1754−1756.
(11) Yamabe, S.; Minato, T.; Osamura, Y. *J. Chem. Soc., Chem. Commun.* **1993**, 450−452.
(12) Ma, N. L.; Wong, M. W. *Eur. J. Org. Chem.* **2000**, 1411−1421.
(13) Arrieta, A.; Cossío, F. P.; Lecea, B. *J. Org. Chem.* **1999**, *64*, 1831−1842.
(14) (a) Rudolf, K.; Spellmeyer, D. C.; Houk, K. N. *J. Org. Chem.* **1987**, *52*, 3708−3710. (b) Niwayama, S.; Kallel, E. A.; Spellmeyer, D. C.; Sheu, C.; Houk, K. N. *J. Org. Chem.* **1996**, *61*, 2813−2825.
(15) (a) Bernardi, F.; Olivucci, M.; Robb, M. A. *Acc. Chem. Res.* **1990**, *23*, 405−412. (b) Houk, K. N.; Li, Y.; Evanseck, J. D. *Angew. Chem., Int. Ed. Engl.* **1992**, *31*, 682−708. (c) Bernardi, F.; Celani, P.; Olivucci, M.; Robb, M. A.; Suzzi-Valli, G. *J. Am. Chem. Soc.* **1995**, *117*, 10531−10536. (d) Haller, J.; Beno, B. R.; Houk, K. N. *J. Am. Chem. Soc.* **1998**, *120*, 6468. (e) Kless, A.; Nendel, M.; Wilsey, S.; Houk, K. N. *J. Am. Chem. Soc.* **1999**, *121*, 4524−4525.
(16) Machiguchi, T.; Hasegawa, T.; Ishiwata, A.; Terashima, S.; Yamabe, S.; Minato, T. *J. Am. Chem. Soc.* **1999**, *121*, 4771−4786.
(17) (a) Moore, H. W.; Hughes, G.; Srinivasachar, K.; Fernandez, M.; Nguyen, N. V.; Schoon, D.; Tranne, A. *J. Org. Chem.* **1985**, *50*, 4231−4238. (b) Fabian, W. M. F.; Kollenz, G. *J. Phys. Org.* **1994**, *7*, 1−8.
(18) Mahajan et al. have reported ab inito and B3LYP calculations on one such system, 1,3-diaza-1,3-butadiene plus ketene, for which the concerted [4 + 2] cycloaddition is favored.[6o]
(19) (a) Birney, D. M.; Wagenseller, P. E. *J. Am. Chem. Soc.* **1994**, *116*, 6262−6270. (b) Birney, D. M. *J. Org. Chem.* **1994**, *59*, 2557−2564. (c) Wagenseller, P. E.; Birney, D. M.; Roy, D. *J. Org. Chem.* **1995**, *60*, 2853−2859. (d) Birney, D. M. *J. Org. Chem.* **1996**, *61*, 243−251. (e) Ham, S.; Birney, D. M. *J. Org. Chem.* **1996**, *61*, 3962−3968. (f) Birney, D. M.; Ham, S.; Unruh, G. R. *J. Am. Chem. Soc.* **1997**, *119*, 4509−4517. (g) Birney, D. M.; Xu, X.; Ham, S.; Huang, X. *J. Org. Chem.* **1997**, *62*, 7114−7120. (h) Shumway, W.; Ham, S.; Moer, J.; Whittlesey, B. R.; Birney, D. M. *J. Org. Chem.* **2000**, *65*, 7731−7739. (i) Shumway, W. W.; Dalley, N. K.; Birney, D. M. *J. Org. Chem.* **2001**, *66*, 5832−5839.

imines.[2,20c,k] For example, when 2-methylacetylketene is generated in the presence of imines, oxazinones are produced as in eq 2.[21] A recent synthesis of β-lactams by Almqvist et al. reported [2 + 2] products from imines and Meldrum's acid derivatives, which are often used as pyrolytic sources of α-oxoketenes. However, these reactions were catalyzed by HCl; thus, there is no requirement for the intermediacy of the ketene.[5o] Sato et al. have also reported that oxazinones can equilibrate upon heating to the β-lactams, possibly through the intermediacy of an α-oxoketene.[20k] Beyond these examples, [2 + 2] cycloadditions are apparently unknown.[2c,20c] Experimental studies on cycloadditions of imidoylketenes are rare due to difficulties in generating these reactive intermediates and also because of competing reactions.[19g]

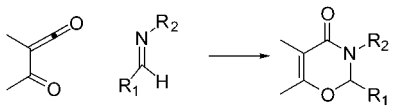

(2)

The addition of formaldehyde to **1b** and **1c** provides a point of comparison with the formaldimine reactions. Theoretical studies predict[19a,e] and experimental studies[19g,h] are consistent with approximately planar, pseudopericyclic pathways for [4 + 2] cycloadditions of **1b** and **1c**. Such reactions are characterized by a disconnection in the cyclic orbital overlap that would be expected for a pericyclic reaction. In the case of **1b** and **1c**, this disconnection is due to the presence of in-plane orbitals on the ketene and carbonyl, as well as the extended out-of-plane π-system. There are three consequences of a pseudopericyclic orbital topology: (1) the transition states can be planar, (2) the reactions can have dramatically lowered, or nonexistent, barriers, and (3) no pseudopericyclic reaction can be forbidden.[19a,c−i,22] These points are all illustrated by the results reported herein.

The above results raise several as yet unanswered questions. What are the factors that control the periselectivity for [4 + 2] or [2 + 2] cycloadditions of conjugated ketenes with imines? The presence of in-plane lone pairs in both **1b** and **1c** raises the possibility of pseudopericyclic overlap in their reactions as contrasted to the lack of an in-plane lone pair on the CH_2 in **1a**; does this play a role in the different periselectivities of these ketenes? Why do ketene−imine cycloadditions follow a different pathway and not utilize the same orbitals as in ketene−alkene cycloadditions? To answer these questions and to deepen our understanding of these reactions, we undertook a density functional theory (DFT) study of these three conjugated ketenes

Scheme 1

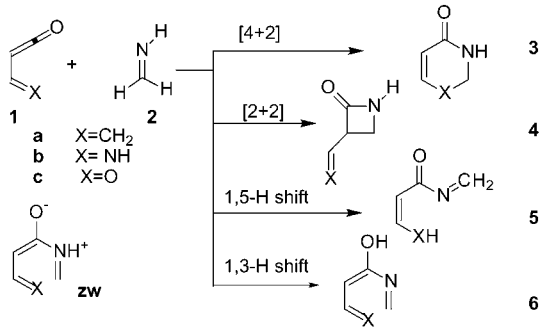

and their reactions with **2**, the simplest imine, to form **3** and **4** (Scheme 1). The choice of **2** as the model system led to some reaction possibilities that would not be possible with an N-substituted imine. In particular, we examined the possibility of pseudopericyclic 1,3- and 1,5-hydrogen shifts in the zwitterionic intermediates (**zw**) to form **5** and **6**.

Computational Methods

The molecular orbital calculations were carried out using Gaussian 94 and Gaussian 98.[23] Geometry optimizations were attempted first at the RHF/3-21G level and then with the B3LYP functional[24a] using the 6-31G* basis set.[24b] Some of the expected complexes and transition structures could not be located at one or both of the levels. When an anticipated transition state or intermediate could not be located at the B3LYP/6-31G* level, a systematic search with constrained distances verified there was no corresponding stationary point; these are summarized in Table S1. There are a large number of possible conformations; only selected structures at the B3LYP/6-31G* level from the lowest energy pathways are presented in Figures 2−5. Geometry optimized structures for all the reactants, intermediates, transition states, and products and at both theoretical levels are shown in the Supporting Information (Figures S1−S9), as are absolute energies (Tables S2−S5). The atom numbering is based on the heavy atoms in the ketene first and then formaldimine (**2**), as shown in Figure 2A. Frequency calculations verified the identity of each stationary point as a minimum or transition state. In some cases, intrinsic reaction coordinate (IRC) calculations were performed to connect the transition states to their respective minima.[25] For selected transition structures, natural bond orbital (NBO) analysis[26] was performed; the results are summarized in Scheme S1. Relative energies, free energies, and the lowest or imaginary frequencies for all structures in the Figures are reported in Tables 1−4.

(20) (a) Barbaro, G.; Battaglia, A.; Giorgianni, P. *J. Org. Chem.* **1987**, *52*, 2, 3289−3296. (b) Danheiser, R. L.; Brisbois, R. G.; Kowalczyk, J. J.; Miller, R. F. *J. Am. Chem. Soc.* **1990**, *112*, 3093. (c) Wentrup, C.; Heilmayer, W.; Kollenz, G. *Synthesis* **1994**, 1219−1248. (d) Sharma, A. K.; Mazumdar, S. N.; Mahajan, M. P. *J. Org. Chem.* **1996**, *61*, 5506−5509. (e) Loebach, J. L.; Bennett, D. M.; Danheiser, R. L. *J. Org. Chem.* **1998**, *63*, 8380−8389. (f) Bennett, D. M.; Okamoto, I.; Danheiser, R. L. *Org. Lett.* **1999**, *1*, 641−644. (g) Sharma, A. K.; Kumar, R. S.; Mahajan, M. P. *Heterocycles* **2000**, *52*, 603−619. (h) Ammann, J. R.; Flammang, R.; Wong, M. W.; Wentrup, C. *J. Org. Chem.* **2000**, *65*, 2706−2710. (i) Trahanovsky, W. S.; Surber, B. W.; Wilkes, M. C.; Preckel, M. M. *J. Am. Chem. Soc.* **1981**, *104*, 6779−6781. (j) Collomb, D.; Doutheau, A. *Tetrahedron Lett.* **1997**, *38*, 1397−1398. (k) Sato, M.; Ogasawara, H.; Yoshizumi, E.; Kato, T. *Chem. Pharm. Bull.* **1983**, *31*, 1902−1909.
(21) Shumway, W. W. *Diastereoselectivity and Reactivity of Oxoketene and Imidoylketene: Investigating the Pseudopericyclic Reaction Mechanism*; Texas Tech University: Lubbock, TX, 2001.
(22) (a) Ham, S.; Birney, D. M. *Tetrahedron Lett.* **1994**, *35*, 8113−8116. (b) Ham, S.; Birney, D. M. *Tetrahedron Lett.* **1997**, *38*, 5925−5928. (c) Birney, D. M.; Xu, X.; Ham, S. *Angew. Chem., Int. Ed.* **1999**, *38*, 189−193. (d) Quideau, S.; Looney, M. A.; Pouységu, L.; Ham, S.; Birney, D. *Tetrahedron Lett.* **1999**, *40*, 615−618.
(23) (a) Frisch, M. J.; Trucks, G. W.; Schlegel, H. B.; Gill, P. M. W.; Johnson, B. G.; Robb, M. A.; Cheeseman, J. R.; Keith, T.; Petersson, G. A.; Montgomery, J. A.; Raghavachari, K.; Al-Laham, M. A.; Zakrzewski, V. G.; Ortiz, J. V.; Foresman, J. B.; Cioslowski, J.; Stefanov, B. B.; Nanayakkara, A.; Challacombe, M.; Peng, C. Y.; Ayala, P. Y.; Chen, W.; Wong, M. W.; Andres, J. L.; Replogle, E. S.; Gomperts, R.; Martin, R. L.; Fox, D. J.; Binkley, J. S.; Defrees, D. J.; Baker, J.; Stewart, J. P.; Head-Gordon, M.; Gonzalez, C.; Pople, J. A. *Gaussian 94*, revision B.3; Gaussian, Inc.: Pittsburgh, PA, 1995. (b) Frisch, M. J.; Trucks, G. W.; Schlegel, H. B.; Scuseria, G. E.; Robb, M. A.; Cheeseman, J. R.; Zakrzewski, V. G.; Montgomery, J. A., Jr.; Stratmann, R. E.; Burant, J. C.; Dapprich, S.; Millam, J. M.; Daniels, A. D.; Kudin, K. N.; Strain, M. C.; Farkas, O.; Tomasi, J.; Barone, V.; Cossi, M.; Cammi, R.; Mennucci, B.; Pomelli, C.; Adamo, C.; Clifford, S.; Ochterski, J.; Petersson, G. A.; Ayala, P. Y.; Cui, Q.; Morokuma, K.; Malick, D. K.; Rabuck, A. D.; Raghavachari, K.; Foresman, J. B.; Cioslowski, J.; Ortiz, J. V.; Stefanov, B. B.; Liu, G.; Liashenko, A.; Piskorz, P.; Komaromi, I.; Gomperts, R.; Martin, R. L.; Fox, D. J.; Keith, T.; Al-Laham, M. A.; Peng, C. Y.; Nanayakkara, A.; Gonzalez, C.; Challacombe, M.; Gill, P. M. W.; Johnson, B. G.; Chen, W.; Wong, M. W.; Andres, J. L.; Head-Gordon, M.; Replogle, E. S.; Pople, J. A. *Gaussian 98*, revision A.6; Gaussian, Inc.: Pittsburgh, PA, 1998.
(24) (a) Becke, A. D. *J. Chem. Phys.* **1993**, *98*, 5648−5652. (b) Hariharan, P. C.; Pople, J. A. *Theor. Chim. Acta* **1973**, *28*, 213.
(25) (a) Fukui, K. *Acc. Chem. Res.* **1981**, *14*, 363−368. (b) González, C.; Schlegel, H. B. *J. Phys. Chem.* **1990**, *94*, 5523.
(26) Weinhold, F.; Carpenter, J. E. *The Structure of Small Molecules and Ions*; Plenum: New York, 1988.

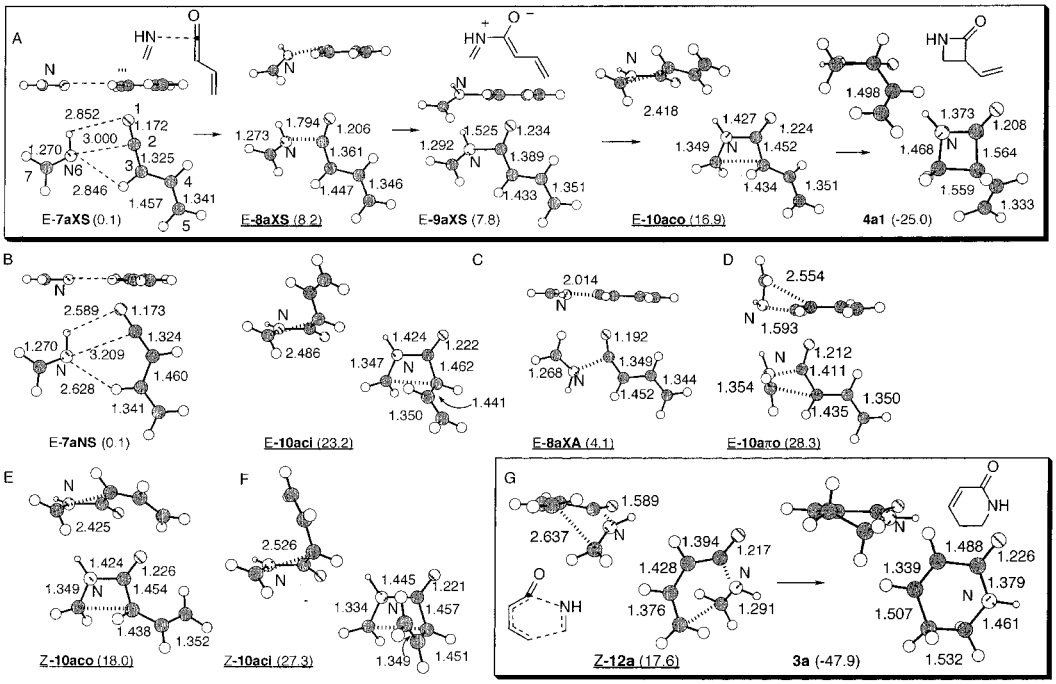

Figure 2. Side and top views of selected B3LYP/6-31G* optimized structures for reactions between **2** and vinylketene (**1a**). Distances shown are in angstroms. Carbons are shaded, hydrogens are open, oxygens are striped, and nitrogens are labeled. "- - -" are close approaches and/or H-bonds; "||||||" are partial bonds. Relative energies are in parentheses in kcal/mol. Lowest energy pathways are boxed. Transition state labels are underlined.

Zero-point vibrational energy corrections have been applied, but have not been scaled. All energies discussed in the paper are at the B3LYP/6-31G*//B3LYP/6-31G* + ZPE level unless otherwise noted. If the potential energy barrier is very low, and the ZPE correction is significant, this treatment of the energies can lead to a barrier less than zero. Because it has been suggested that DFT calculations can underestimate barriers' heights by a few kcal/mol,[27] such a situation should not be over-interpreted, but can be taken as an indication of the lack of a significant barrier.

Density functional theory using the B3LYP functional (the hybrid three-parameter functional developed by Becke[24a]) was the primary theoretical method utilized in this work. This method has been shown to give reliable transition structure geometries and energies for a variety of pericyclic reactions.[28] In some cases, it gives more consistent results than MP2 calculations, with much less computer time.[28f] To help confirm that the B3LYP/6-31G* calculations are appropriate for ketenes, the experimental geometry of ketene was compared with that calculated at the B3LYP/6-31G* (this work), MP2(FU)/6-31G*,[12] and MP2(FC)/6-31G* (this work) levels. The B3LYP geometries are closer to the experimental than are the MP2 geometries (see Supporting Information, Figure S10). Ma and Wong[12] provide additional comparisons that support the use of B3LYP calculations for ketenes. For these particular reactions, we reoptimized several structures with the 6-311+G** basis set (*Z*-8**bNS**, *Z*-**9bNS**, *Z*-**10bco**, *Z*-**11bπo**, *Z*-**11b**, *Z*-**12b**, Figure S12, Table S6A,B). There were no significant differences in the geometries or relative energies. An attempt was also made to perform unrestricted B3LYP calculations on these structures, to see if biradical contributions to the transition states or intermediates were important; in all cases, these converged to the closed shell wave function (Table S6C).

It might be expected that solvation would be important for polar species such as the zwitterions. However, Cossío[6m,29] and Sordo[6g,k] have reported numerous calculations on cycloadditions of ketenes and related species using theoretical models for solvation; in their treatment, solvation leads to only a minor difference in the structures and energies. Nevertheless, calculations using the self-consistent isodensity polarized continuum model (SCI-PCM) of solvation[30] ($e = 9.08$) were performed on selected structures (**3b**, **4b1**, **4b2**, *Z*-**9bNS**, *Z*-**10bco**, *Z*-**11bπo**, *Z*-**11b**, *Z*-**12b**, Table S6D,E). Solvation stabilized each structure by between 5.0 and 8.5 kcal/mol; however, there were no significant differences in the relative energies. In conclusion, the B3LYP/6-31G* level of theory used in this study appears to be an appropriate model for the reactions studied herein.

Results and Discussion

Conformations of Vinylketene (1a), Imidoylketene (1b), and Formylketene (1c). The geometries and conformations of these conjugated ketenes have been extensively studied at a variety of theoretical levels.[19b,e,31] For consistency, we recalculated them at the B3LYP/6-31G* level. Our results are qualitatively consistent with those obtained at other levels. Specifically, we calculate that the *s*-*E*-conformation of **1a** is more stable than the *s*-*Z* by 1.7 kcal/mol (Table 1). For **1b**,

(27) (a) Lynch, B.; Fast, P. L.; Harris, M.; Truhlar, D. G. *J. Phys. Chem. A* **2000**, *104*, 4811−4815. (b) McKee, M. L.; Shevlin, P. B.; Zottola, M. *J. Am. Chem. Soc.* **2001**, *123*, 9418−9425.
(28) Selected references include 6n, 27b, and (a) Curtiss, L. A.; Raghavachari, K.; Redfern, P. C.; Pople, J. A. *J. Chem. Phys.* **1997**, *106*, 1063−1079. (b) Singleton, D. A.; Merrigan, S. R.; Liu, J.; Houk, K. N. *J. Am. Chem. Soc.* **1997**, *119*, 3385−3386. (c) Hrovat, D. A.; Chen, J.; Houk, K. N.; Borden, W. T. *J. Am. Chem. Soc.* **2000**, *122*, 7456−7460. (d) Cossío, F. P.; Arrieta, A.; Lecea, B.; Alajarín, M.; Vidal, A.; Tovar, F. *J. Org. Chem.* **2000**, *65*, 3633−3643. (e) Koch, W.; Holthausen, M. C. *A Chemist's Guide to Density Functional Theory*; Wiley-VCH: New York, 2000. (f) Birney, D. M. *J. Am. Chem. Soc.* **2000**, *122*, 10917−10925.
(29) Lecea, B.; Arrieta, A.; Roa, G.; Ugalde, J. M.; Cossío, F. P. *J. Am. Chem. Soc.* **1994**, *116*, 9613−9619.
(30) McWeeny, R. *Rev. Mod. Phys.* **1960**, *32*, 335.
(31) (a) Allen, A. D.; Gong, L.; Tidwell, T. T. *J. Am. Chem. Soc.* **1990**, *112*, 6396−6397. (b) Nguyen, M. T.; Ha, T.; More O'Ferrall, R. A. *J. Org. Chem.* **1990**, *55*, 3251−3256. (c) Wong, M. W.; Wentrup, C. *J. Org. Chem.* **1994**, *59*, 5279−5285. (d) Janoschek, R.; Fabian, W. M. F.; Kollenz, G.; Kappe, O. C. *J. Comput. Chem.* **1994**, *15*, 132−143. (e) McAllister, M. A.; Tidwell, T. T. *J. Org. Chem.* **1994**, *59*, 4506−4515. (f) Eisenberg, S. W. E.; Kurth, M. J.; Fink, W. H. *J. Org. Chem.* **1995**, *60*, 3736−3742. (g) Kappe, C. O.; Wong, M. W.; Wentrup, C. *J. Org. Chem.* **1995**, *60*, 1686−1695. (h) Bibas, H.; Wong, M. W.; Wentrup, C. *J. Am. Chem. Soc.* **1995**, *117*, 9582−9583. (i) Bibas, H.; Wong, M. W.; Wentrup, C. *Chem.-Eur. J.* **1997**, *3*, 237−248. (j) Badawi, H. M.; Förner, W.; Al-Saadi, A. *J. Mol. Struct. (THEOCHEM)* **2000**, *505*, 19−30.

Table 1. Calculated Relative Energies (kcal/mol), Relative Energies with Zero-Point Vibrational Energy Corrections (ZPE, kcal/mol), Low or Imaginary Frequencies (cm^{-1}), and Free Energies (kcal/mol) for Structures Related to the Addition Reaction of Vinylketene (**1A**) and Formaldimine (**2**) at the B3LYP/6-31G* Level

structure	relative energy[a]	relative energy + ZPE	low frequencies	relative free energy	structure	relative energy[a]	relative energy + ZPE	low frequencies	relative free energy
Z-**1a** + **2**	5.7	4.6	74.4; 1084.1	−4.2	*E*-**10aci**	21.7	23.2	394.9i	26.9
E-**1a** + **2**	3.9	2.9	28.9; 1084.1	−5.4	*E*-**7aNA**	0.3	0.2	27.7	−0.3
Z-**7aNS**	2.8	2.5	17.4	1.0	*E*-**8aNA**	5.0	5.9	257.4i	8.6
Z-**7aNA**	3.0	2.8	22.8	1.5	*E*-**9aNA**	0.3	2.6	102.4	5.8
Z-**8aNA**	6.7	7.4	189.6i	10.3	*E*-**7aXS**	0.3	0.1	21.1	−0.9
Z-**9aNA**	−0.3	2.3	124.7	6.0	*E*-**8aXS**	7.2	8.2	242.4i	10.8
Z-**10aci**	26.0	27.3	79.7	30.9	*E*-**9aXS**	5.9	7.8	120.2	10.8
Z-**7aXS**	2.2	1.8	19.6	0.4	*E*-**7aXA**	0.0	0.0	34.4	0.0
Z-**8aXS**	8.9	9.9	246.2i	12.5	*E*-**8aXA**	3.2	4.1	221.8i	6.7
Z-**9aXS**	7.2	9.3	92.1	12.4	*E*-**9aXA**	−3.2	−0.7	98.8	2.6
Z-**7aXA**	1.8	1.7	25.6	1.1	*E*-**10aco**	15.2	16.9	340.1i	20.5
Z-**8aXA**	4.8	5.6	214.8i	8.3	*E*-**10aπi**	29.8	31.1	437.6i	34.6
Z-**9aXA**	−2.0	0.6	88.2	4.1	*E*-**10aπo**	27.1	28.3	406.0i	31.7
Z-**10aco**	16.2	18.0	334.8i	21.8	**3a**	−53.6	−47.9	137.7	−43.5
Z-**10aπi**	29.2	31.0	319.6i	35.0	**4a1**	−28.8	−25.0	90.8	−21.6
Z-**10aπo**	28.7	29.9	397.7i	33.4	**4a2**	−29.5	−25.8	84.4	−22.5
Z-**12a**	15.9	17.6	270.9i	15.3	**4a3**	−29.0	−25.1	79.7	−21.7
E-**7aNS**	0.3	0.1	25.5	−0.7					

[a] Energies are relative to *E*-**7aXA**, the most stable complex.

Table 2. Calculated Relative Energies (kcal/mol), Relative Energies with Zero-Point Vibrational Energy Corrections (ZPE, kcal/mol), Low or Imaginary Frequencies (cm^{-1}), and Free Energies (kcal/mol) for Selected Structures Related to the Addition Reaction of Imidoylketene (**1b**) and Formaldimine (**2**) at the B3LYP/6-31G* Level

structure	relative energy[a]	relative energy + ZPE	low frequencies	free energy
E-*s*-*Z*-**1b** + **2**	4.7	3.8	149.1; 1084.1	−4.8
Z-*s*-*Z*-**1b** + **2**	6.5	5.5	133.0; 1084.1	−3.3
E-*s*-*E*-**1b** + **2**	4.3	3.3	147.0; 1084.1	−5.2
Z-*s*-*E*-**1b** + **2**	4.6	3.5	132.9; 1084.1	−5.2
3b	−45.4	−40.0	155.2	−35.9
4b1	−28.6	−24.8	62.4	−21.6
4b2	−27.3	−23.6	89.0	−20.6
E-**7bXA**	0.0	0.0	36.3	0.0
Z-**8bNS**	5.5	6.2	61.7i	7.4
Z-**9bNS**	0.5	3.1	70.2	6.1
E-**10bco**	18.5	20.2	386.4i	23.5
E-**10bci**	22.4	24.1	409.5i	27.6
Z-**10bco**	23.4	24.9	374.2i	28.2
Z-**10bci**	20.9	22.9	329.1i	28.2
E-**10bπo**	29.5	30.8	464.9i	34.1
Z-**11b**	1.8	4.2	200.8i	7.8
Z-**12b**	7.4	9.2	218.0i	12.2

[a] Energies are relative to *E*-**7bXA**, the most stable complex.

there are four minima, because the imide bond can also be *Z* or *E*. At the B3LYP/6-31G* level, the *Z*-*s*-*Z*, *E*-*s*-*Z*, and *Z*-*s*-*E* structures are 2.2, 0.5, and 0.2 kcal/mol, respectively, above that of the *E*-*s*-*E* structure (Table 2). For **1c**, all calculations predict the two conformations to be similar in energy, but at this level, the *s*-*Z*-conformation is 0.2 kcal/mol above the *s*-*E*-conformation. Because the different conformations of **1a**, **1b**, and **1c** are close in energy, we have considered both *s*-*Z*- and *s*-*E*-conformations in this work. For clarity and simplicity in the discussion below, the *E*-isomer of the imine in **1b** will be assumed, and thus *Z* and *E* will be used to refer only to the *s*-*Z*- and *s*-*E*-conformations.

Complexes between Formaldimine (2) and Ketenes 1a, 1b, and 1c. Gas-phase van der Waals complexes have been calculated for ketenes with other reagents.[19a,32] The complexes between ketene and both ethylene and acetylene have been characterized by microwave spectroscopy.[33] Both experiment and calculation agree that complexation occurs in the plane of the ketene, with the interaction of a weakly nucleophilic π-bond with the in-plane LUMO of ketene. The anticipated in-plane complexes between **1a**, **1b**, and **1c** and the nucleophilic imine **2** were indeed found (Figures 2A, 2B, S1, S4, S7).

Scheme 2

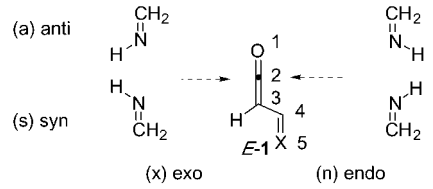

For both *E*- and *Z*-conformers of the conjugated ketenes **1a**, **1b**, **1c**, these complexes with formaldimine (**2**) were systematically explored. There has not been a consistent nomenclature to describe the geometries of attack on the ketene, but the descriptions outlined in Scheme 2 are in general consistent with other discussions[6b,k,n] and will be used in the remainder of this paper. The addition of **2** can occur either exo (x) or endo (n) to the substituent on the ketene (**1**), and the imine **2** can be oriented either syn (s) or anti (a) to the β-carbon. Finally, there are both *E*- and *Z*-conformers of the conjugated ketenes (see above). Thus, there are eight possible geometries for coplanar addition of the ketenes **1** and formaldimine **2**, and, for example, *E*-**7aXS** is the exo-syn complex of *E*-**1a** with **2**, as shown in Figure 2. Indeed, van der Waals complexes between **1** and **2** were located for most, but not all of these possibilities (Tables 1−3 and Supporting Information, Figures S1, S4, S7 and Tables S2−S4). These complexes are in shallow minima, bound by between 2.9 kcal/mol (*E*-**7aXA**) and 3.9 kcal/mol (*E*-**7cXA**, Tables 1, 2, 3). Thus, equilibration between them can readily occur by fragmentation/recombination. The *E*-**1** complexes are of nearly equal energy, within 0.4 kcal/mol of each other. The *Z*-**1**

(32) (a) Sung, K.; Tidwell, T. T. *J. Am. Chem. Soc.* **1998**, *120*, 3043−3048. (b) Couturier-Tamburelli, I.; Aycard, J.-P.; Wong, M. W.; Wentrup, C. *J. Phys. Chem. A* **2000**, *104*, 3466−3471.
(33) (a) Gillies, C. W.; Gillies, J. Z.; Lovas, F. J.; Suenram, R. D. *J. Am. Chem. Soc.* **1993**, *115*, 9253−9235. (b) Lovas, F. J.; Suenram, R. D.; Gillies, C. W.; Gillies, J. Z.; Fowler, P. W.; Kisiel, Z. *J. Am. Chem. Soc.* **1994**, *116*, 5285−5294.

Table 3. Calculated Relative Energies (kcal/mol), Relative Energies with Zero-Point Vibrational Energy Corrections (ZPE, kcal/mol), Low or Imaginary Frequencies (cm^{-1}), and Free Energies (kcal/mol) for Selected Structures Related to the Addition Reaction of Formylketene (**1c**) and Formaldimine (**2**) at the B3LYP/6-31G* Level

structure	relative energy[a]	relative energy + ZPE	low frequencies	free energy
Z-**1c** + **2**	5.2	4.1	143.8; 1084.1	−4.5
E-**1c** + **2**	5.0	3.9	156.2; 1084.1	−4.7
3c	−32.6	−27.5	130.7	−23.5
4c1	−25.0	−21.6	83.7	−18.6
4c2	−23.5	−20.2	114.9i	−15.7
E-**7cXA**	0.0	0.0	42.2	0.0
Z-**8cNS**	3.5	3.2	466i	5.5
Z-**9cNS**	−1.1	1.4	71.2	4.3
Z-**10cco**	25.3	26.6	418.4i	29.8
E-**10cco**	22.2	23.6	429.8i	26.8
Z-**10cci**	21.2	23.0	342.8i	26.6
E-**10cci**	21.7	23.3	211.0i	26.8
Z-**10cπi**	29.8	31.5	501.1i	35.0
E-**10cπi**	32.5	33.7	530.4i	36.8
Z-**11c**	−0.2	2.1	174.0i	5.6
Z-**12c**	4.9	6.6	197.8i	9.6

[a] Energies are relative to *E*-**7cXA**, the most stable complex.

complexes with **2** are generally higher in energy by 0.2−2.8 kcal/mol, reflecting the higher energy of the *Z*-conformation and, in some cases, steric congestion with the vinyl group. The latter leads to slightly nonplanar complexes for *Z*-**7aNA** and *E*-**7cXS** and significantly nonplanar complexes for *Z*-**7bNS**, *Z*-**7cNS**, and *Z*-**7cNA**. Of the four *E*-complexes, the exo-anti (**XA**) complexes are consistently the most stable.

Addition of Formaldimine (2) to Vinylketene (1a). We begin the discussion with a consideration of the stepwise [2 + 2] cycloadditions of **2** with **1a** (Figures 2A, 2B, 2E, 2F, S2, and S3). When a stable zwitterionic intermediate (**9**) is formed, it has a low barrier (via **8**) to fragmentation back to the complex. Subsequent electrocyclization forms the four-membered ring products in the rate-determining step (eq 3). These conrotatory transition structures (**10**) can have the substituent rotate either inward or outward and are designated with the suffixes **ci** or **co** respectively.

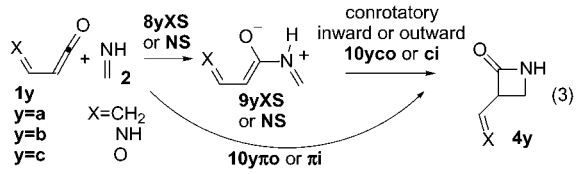

The lowest energy intermediates are the exo-anti intermediates, for example, *E*-**9aXA** (−0.7 kcal/mol). The other zwitterions are apparently destabilized by steric interactions. In particular, the endo-syn zwitterions *Z*- and *E*-**9aXS** are twisted slightly out-of-plane (gauche) and are significantly higher in energy (9.3 and 7.8 kcal/mol, respectively). Structures corresponding to *Z*- and *E*-**9aNS** were not minima but were calculated to dissociate to the van der Waals complexes *Z*- and *E*-**7aNS**, respectively. It is possible that solvation would stabilize these structures sufficiently to make them weakly bound intermediates.[6g] Although the most stable, the anti zwitterions are not directly on the reaction pathways. There was originally some confusion in this regard. Both Cossío[6b,d] and Sordo[6a,c,g] described the cycloaddition of ketene and formaldimine as first forming the anti zwitterion, and then the electrocyclization occurring from this conformation. Sordo subsequently revised this picture, indicating that the cyclization occurred from the syn (gauche) conformation, as determined by IRC calculations.[6k,p] We also performed IRC calculations that connected the conrotatory transition structure *E*-**10aco** to the syn zwitterion *E*-**9aXS**. Computational attempts to locate a rotational transition state connecting *E*-**9aXS** and *E*-**9aXA** led to fragmentation to the van der Waals complexes *E*-**7aXS** and *E*-**7aXA**.[34] The weakness of the zwitterions is also reflected in the long C2−N6 bonds (1.484−1.532 Å). Clearly, there is a facile equilibration via fragmentation between all the zwitterions and the van der Waals complexes.

Of the [2 + 2] addition pathways, the lowest overall calculated energy barrier of 16.9 kcal/mol is for the conrotatory, outward electrocyclization via *E*-**10aco** from the exo-syn zwitterion, *E*-**9aXS**, as shown in Figure 2A.[35] In agreement with previous results,[6a−e,g,k,m,n] it is the torquoselectivity of this ring closure that leads to the stereoselective formation of the products. This barrier is sufficiently low that the reaction could take place readily at room temperature, in agreement with experimental observations.[20a,d,g] Sordo et al. calculated a barrier of 21.3 kcal/mol (MP2/6-31G*, no ZPE correction) for ketene plus formaldimine.[6a] While the levels of calculation are different, the barriers are comparable; the vinyl substituent may slightly lower the barrier for the [2 + 2] cycloaddition.

The overall barrier for the similar stepwise [2 + 2] cycloaddition from the *Z*-conformation of **1a** is only slightly higher, 18.0 kcal/mol for *Z*-**10aco** (Figure 2E). These electrocyclizations exhibit significant torquoselectivity; the transition structures with inward rotation *E*-**10aci** and *Z*-**10aci** (Figure 2B,F) have higher barriers of 23.2 and 27.3 kcal/mol, respectively. This is in agreement with the original work of Houk et al. who calculated that alkene substituents prefer to rotate outward in cyclobutene ring openings.[14a]

Four other transition structures for [2 + 2] cycloadditions between **1a** and **2** were located. The lowest energy structure (*E*-**10aπo**) is shown in Figure 2D; the others (designated as **πo** and **πi**) are shown in Figures S2 and S3. While this is of considerably higher energy (28.3 kcal/mol) than the stepwise pathway via *E*-**10aco** (16.9 kcal/mol), it is nevertheless of significance. Similar structures have been the subject of considerable controversy. In their calculations on the fluoroketene plus imine cycloaddition, Xu, Fang, and Fu reported a structure that according to IRC calculations did not connect to a zwitterion.[6f,i] This conclusion was disputed by Sordo et al.[6h] who have previously calculated electrocyclic transition structures related to *Z*- and *E*-**10aco**.[6c,g] We also performed an IRC calculation beginning from *E*-**10aπo**, and this connected to the cyclobutenedione **4a1** (Figure S3) but not to any of the zwitterionic intermediates. It thus appears that the results of both Xu et al. and of Sordo et al. are correct; there are simply two

(34) Cossío reported locating a transition structure at the semiempirical AM1 level for a similar rotation in the cycloaddition of ketene with imine.[6b] However, in the current work (B3LYP/6-31G*), constraining the C2−N5 distance to 1.525 Å gave a quasi-transition structure with a relative energy of 14.4 kcal/mol, higher in energy than the dissociation/recombination pathway.

(35) For thermal, conrotatory cyclobutene ring openings see: (a) Marvell, E. N. *Thermal Electrocyclic Reactions*, 1st ed.; Academic Press: New York, 1980. (b) Spellmeyer, D. C.; Houk, K. N. *J. Am. Chem. Soc.* **1988**, *110*, 3412−3416.

transition structures and two independent pathways. As discussed above, Sordo et al. later described this transition state as disrotatory.[6k] While this indeed appears disrotatory at first inspection, there are two difficulties with this designation. As argued above, a forbidden transition structure would not be expected to be well described by the single determinant (RHF) wave functions used by both Xu and Sordo. Yet more importantly, this is a highly asynchronous, but concerted transition structure, in which the C2−N6 is not fully formed (1.593 Å). A closer inspection of the geometry reveals that it is more related to the ketene plus ethylene cycloaddition transition structure.[10−12] (Side and top views of the transition states for ketene plus ethylene and ketene plus **2** are shown in Figure S11.) Finally, the barrier of 28.3 kcal/mol for *E*-**10a**π**o** is comparable to that calculated for ketene plus ethylene (28.9 kcal/mol, G2(MP2) level).[12] Both the geometry and the barrier heights suggest that there is nothing unusual about these transition structures (*Z*- and *E*-**10a**π**o** and *Z*- and *E*-**10a**π**i**). Rather, the imine π-bond is being utilized in the same fashion as the π-bond of ethylene. The geometry and NBO analysis of *E*-**10a**π**o** are in accord with the interpretation of Yamabe that there are two separate orbital interactions, primarily donation from the imine π to the in-plane ketene π^* and secondarily from the out-of-plane ketene π to the imine π^*. To put this in a broader context, the orbital disconnection between the two ketene orbitals (Figure 1A) means that these cycloadditions are pseudopericyclic. However, the conrotatory transition structures (*Z*- and *E*-**10aco** and *Z*- and *E*-**10aci**) are all lower in energy, and thus the stepwise pathways are followed.

A concerted, asynchronous transition structure for the [4 + 2] cycloaddition was located (*Z*-**12a**, eq 4, Figure 2G, Table 1). This nonplanar geometry is similar to other pericyclic Diels−Alder reactions with suprafacial orbital interactions.[15] However, the imine lone pair is oriented toward the ketene carbon (C2). This differs from the exo-lone-pair effect found by Houk and McCarrick for Diels−Alder reaction with butadiene,[36] presumably because of the attraction between the lone pair and the ketene in-plane LUMO in *Z*-**12a**. Attempts to locate a stepwise transition structure (see below for **1b** and **1c**) led only to the concerted structure.

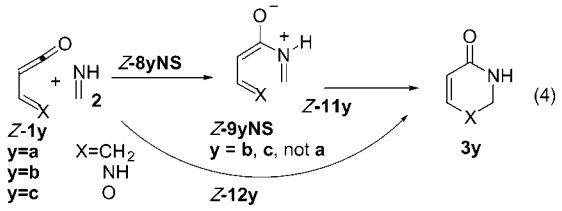

Comparing the energies of the various transition states, the stepwise [2 + 2] pathway is favored (the lowest barrier is 16.9 kcal/mol, *E*-**10aco**). This result is in agreement with the experimental results obtained by Barbaro et al.[20a] and Sharma et al.,[20d,g] in which [2 + 2] products are formed in reactions of unconstrained vinylketenes with imines. However, the concerted [4 + 2] pathway is not much higher in energy (17.6 kcal/mol, *Z*-**12a**) than the [2 + 2], and it is the lowest pathway for the *s*-*Z* conformation; the stepwise [2 + 2] via *Z*-**10aco** is 18.0 kcal/mol. Thus, we predict that for a vinylketene constrained to a *Z*-geometry, the [4 + 2] could be competitive; this may be relevant to the [4 + 2] cycloaddition of silylvinylketene with imines observed by Danheiser et al.,[20f] although silyl substitution significantly perturbs ketene reactivity.[2c]

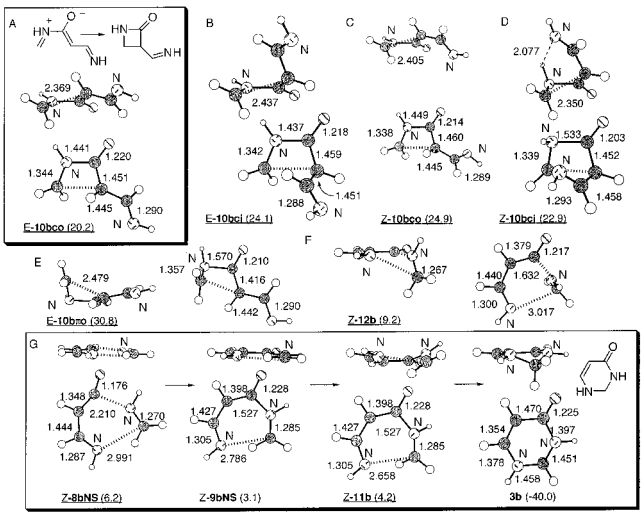

Figure 3. Side and top views of selected B3LYP/6-31G* optimized structures on the low energy pathways for reactions between **2** and imidoylketene (**1b**). See Figure 2 for key.

Addition of Formaldimine (2) to Imidoylketene (1b). Because of the difficulties with the preparation of imidoylketenes, their reactions with imines are apparently unknown.[2c] The results below suggest that such reactions should be possible. A closely related reaction of benzoimidoylketene from isatoic anhydride with an imine has been reported.[37]

Seven complexes between imidoylketene (**1b**) and **2** were located; the *E*-conformations are again more stable, and *E*-**7bXA** is the most stable (see Supporting Information, Figure S4 and Table S3). The missing eighth complex would be *Z*-**7bNA**; however, attempts to optimize this structure gave *Z*-**7bXA**. Presumably, lone pair repulsion between the two nitrogens destabilizes the endo-anti conformation of what would be *Z*-**7bNA**.

Two pathways for [2 + 2] cycloadditions were again calculated, stepwise and concerted (eq 3). These geometries and energies were similar to those calculated for vinylketene **1a**. Thus, of the four stepwise pathways for a [2 + 2] (Figures 3A−D, S5, and S6), *E*-**10bco** was the highest barrier (20.2 kcal/mol) on the lowest energy pathway. The zwitterion *Z*-**9bNA** is exceptionally stabilized (−12.6 kcal/mol); there is a hydrogen bond between N6H and N5. Although this hydrogen bond would not be present in any substituted imine, this structure is of relevance to the facile 1,5-hydrogen shifts reported below. The torquoselectivity was more modest than in the case of vinylketene (**1a**); *E*-**10bci** had a barrier of 24.1 kcal/mol, in accord with Houk's results for 2-iminocyclobutene.[14b] For the *Z*-conformation, the inward transition structure *Z*-**10bci** (22.9 kcal/mol) was lower in energy than the outward structure *Z*-**10bco** (24.9 kcal/mol). This again is a consequence of the choice of **2** as the model imine; there is a hydrogen bond between N6H and N5, as evidenced by substantial pyramidalization of N6 and

(36) McCarrick, M. A.; Wu, Y.-D.; Houk, K. N. *J. Am. Chem. Soc.* **1992**, *114*, 1499−1500.

(37) Staiger, R. P.; Moyer, C. L.; Pitcher, G. R. *J. Chem. Eng. Data* **1963**, *8*, 454−456.

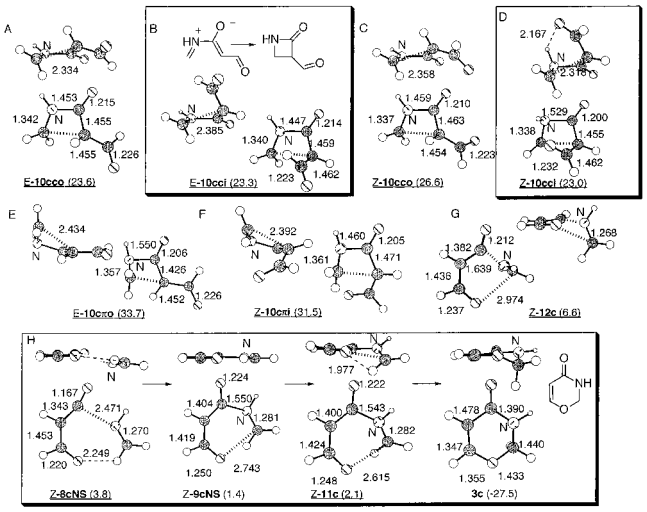

Figure 4. Side and top views of selected B3LYP/6-31G* optimized structures on the low energy pathways for reactions between **2** and formylketene (**1c**). See Figure 2 for key.

stabilization of this structure. This would not be possible with an N-substituted imine.

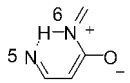

***Z*-9bNA**

Again, four concerted transition structures were located (Figures S5 and S6). The lowest energy was *E*-**10bπo** (30.8 kcal/mol, Figure 3E). These geometries are again very similar to the highly asynchronous, but concerted, cycloaddition of ketene with ethylene. The barriers for both [2 + 2] pathways are slightly higher than those calculated for **1a**. This may reflect the greater stability of imidoylketene (**1b**) versus vinylketene (**1a**)[31e] and/or the greater exothermicity of the reaction of vinylketene (**1a**); the formation of **4a2** is 25.8 kcal/mol exothermic, while the formation of **4b1** is 24.8 kcal/mol exothermic.

However, the formation of the six-membered ring **3b** was calculated to be much more facile for **2** + **1b** than for **1a**. We calculated two low energy pathways (eq 4, Figure 3F and G). The concerted [4 + 2] pathway via *Z*-**12b** has a barrier of only 9.2 kcal/mol. This is remarkably low when compared either to the [4 + 2] cycloaddition of **1a** and **2** (via *Z*-**12a**) or to a hydrocarbon Diels−Alder reaction.[15b,38] Such low barriers are often found for pseudopericyclic reactions.[19d,f,28f,39] Furthermore, the geometry is essentially planar at the ketene (C2) in contrast to the suprafacial−suprafacial geometry of a hydrocarbon Diels−Alder.[15b,38,40] Rather, this geometry is very similar to the pseudopericyclic geometries calculated for the cycloadditions of **1b** and **1c** with carbonyl compounds and described as pseudopericyclic.[19a,e,g,h] Figure 5A shows the pseudopericyclic orbital topology of this transition state, based on the geometry and the NBO analysis (Scheme S1). Experimental support for

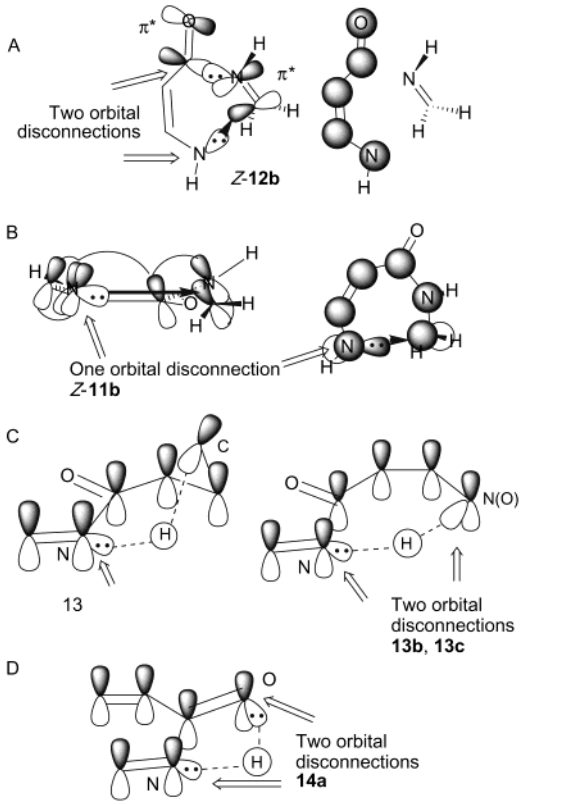

Figure 5. Pseudopericyclic orbital interactions in reactions of **1b**, based on NBO analysis. Note that both side and top views of p-orbitals are shown in A and B. (A) The two orbital disconnections in the [4 + 2] cycloaddition *Z*-**12b**. For clarity, the in-plane and out-of-plane orbitals are shown separately. (B) The single orbital disconnection in the electrocyclization *Z*-**11b**. (C) Orbital disconnections in the 1,5-hydrogen shift **13a**, **13b**, and **13c**. (D) Orbital disconnections in the 1,3-hydrogen shift **14a**, **14b**, and **14c**.

planar, pseudopericyclic transition states is found in the ground-state distortions in the X-ray crystal structure of the camphorketene dimer that prefigures such a reaction.[19i]

The other [4 + 2] pathway is stepwise, with rate-determining nucleophilic attack of the imine nitrogen on C_2 of the ketene via a planar transition structure *Z*-**8bNS** with a barrier of 6.2 kcal/mol. This barrier is comparable to the other barriers for the formation of the zwitterions, although there is some steric crowding in the planar zwitterion *Z*-**9bNS** (3.1 kcal/mol). This intermediate then undergoes very facile electrocyclic ring closure via *Z*-**11b** to give the six-membered product (**3b**, eq 4). The barrier for this reaction is remarkably low, only 1.1 kcal/mol from the zwitterion (*Z*-**9bNS**) to the transition structure (*Z*-**11b**). In fact, the formation of the zwitterion is calculated to be the rate-determining step (*Z*-**8bNS**, 6.2 kcal/mol). Again, such a low barrier is indicative of a pseudopericyclic reaction. As a six-electron process, this would be predicted to be disrotatory.[8] Both the CH_2 (C7) and the NH (N5) are indeed twisted out of the molecular plane in a disrotatory fashion. However, this twisting is slight; the geometry about the C4−N5 imide bond is almost perfectly planar, and the lone pair points directly at C7. (The C3−C4−N5−NH and C3−C4−N5−C7 dihedral angles are 174.8° and 7.2°, respectively.) This planarity and the NBO analysis (see Scheme S1) both indicate a pseudopericyclic orbital topology with a single disconnection at N5, as shown in Figure 5B.[19f] The transition structure *Z*-**11b** is quite early, with the forming N5−C7 bond 2.658 Å long. Overall,

(38) Sauer, J.; Sustmann, R. *Angew. Chem., Int. Ed. Engl.* **1980**, *19*, 779−807.
(39) (a) Fabian, W. M. F.; Bakulev, V. A.; Kappe, C. O. *J. Org. Chem.* **1998**, *63*, 5801. (b) Fabian, W. M. F.; Kappe, C. O.; Bakulev, V. A. *J. Org. Chem.* **2000**, *65*, 47−53. (c) Alajarín, M.; Vidal, A.; Sánchez-Andrada, P.; Tovar, F.; Ochoa, G. *Org. Lett.* **2000**, *2*, 965−968.
(40) For recent X-ray crystallographic evidence for the geometry of the Diels−Alder transition state, see: Pool, B. R.; White, J. M. *Org. Lett.* **2000**, *2*, 3505−3507.

this stepwise process has a slightly lower (by 3.0 kcal/mol) barrier for the formation of **3b** as compared to the concerted process. Because the stepwise formation of the six-membered ring is calculated to have a very low energy barrier (6.2 kcal/mol), the [2 + 2] cycloadditions of *E*- or *Z*-**1b** with **2** (eq 3) are predicted not to be competitive. To the best of our knowledge, there is only one example of a benzoimidoylketene reacting with an imine;[37] this gave a [4 + 2] product. Other examples are currently under investigation in our laboratory.

The transition structure *Z*-**11b** is closely related to the electrocyclization of 1-aza-1,3,5-hexadiene that has been studied by Rodríguez-Otero[41a] and later by Houk et al.[41b] As Rodríguez-Otero recognized, the transition structure for this reaction is planar on the imine and is qualitatively different from the hydrocarbon electrocyclization. Houk suggested a very similar orbital analysis to Figure 5B, but did not place it in the broader context of pseudopericyclic reactions. The very low barrier height of *Z*-**11b** can be understood in the context of the Hammond postulate[42] by comparing the exothermicities of the reactions. Formation of **3b** is 40.0 kcal/mol exothermic, while ring closure of 1-aza-1,3,5-hexadiene is 7.1 kcal/mol endothermic, with a barrier of 27.7 kcal/mol.[41]

Addition of Formaldimine (2) to Formylketene (1c). Formaldimine (**2**) and formylketene (**1c**) are similar in that both have an in-plane lone pair as well as an out-of-plane π-system. All eight expected complexes were located; the *E*-complexes are, in general, more stable, and *E*-**7cXA** has the lowest energy (see Supporting Information, Figure S7 and Table S4).

Transition structures for the two [4 + 2] pathways, concerted and stepwise, were located (eq 4 and Figure 4G and H). These are qualitatively similar to those of the addition of **2** to **1b**. In particular, the concerted [4 + 2] transition structure (*Z*-**12c**, 6.6 kcal/mol) is close to planar (particularly at C2); the NBO analysis (Scheme S1) also indicates this is pseudopericyclic. For the stepwise addition, the initial formation of the zwitterion is again rate determining (*Z*-**8cNS**, 3.8 kcal/mol) and has a lower overall barrier than does the concerted pathway (6.6 kcal/mol, *Z*-**12c**). The electrocyclic ring closure on the stepwise pathway (*Z*-**11c**), although it had residual disrotatory motion, is again close to planar (the C3−C4−O5−C7 dihedral angle is 1.6°), and is therefore also pseudopericyclic with one orbital disconnection at O7, as further evidenced by the NBO analysis (Scheme S1). It also has a very low barrier from the zwitterion (*Z*-**9cNS**, 0.7 kcal/mol) again consistent with a pseudopericyclic reaction.

The [2 + 2] cycloadditions (eq 3, Figures 4A−F, S8, and S9 and Tables 3 and S4) again have significantly higher energy barriers than do the [4 + 2]. On the basis of Houk's work,[14b] the formyl substituent is expected to show significant torquoselectivity for inward rotation; for both *E*- and *Z*-conformations, inward rotation is indeed favored. The lowest energy transition structure is *Z*-**10cci** (23.0 kcal/mol), conrotatory with inward rotation. Again, the *Z*-conformation appears to be artificially stabilized by a hydrogen bond between O5 and N6H (2.167 Å), and N6 is pyramidalized. This hydrogen bond would not be possible in an N-substituted imine. However, the transition structure *E*-**10cci** lacks this hydrogen bond and yet is almost of equal energy (23.3 kcal/mol); it is also conrotatory, with inward rotation.

As before, the concerted transition structures have higher energies (31.5 kcal/mol, *Z*-**10cπi** and 33.7 kcal/mol, *E*-**10cπo**, Figure 4E and F). The barriers for both the stepwise and concerted [2 + 2] cycloadditions are slightly higher than for the corresponding reactions of **1a** and **1b**, reflecting the greater stability of **1c**.[31e] Overall, these results are consistent with the [4 + 2] cycloaddition products experimentally observed in the reactions of acetylketene with imines.[2,20c,k,21]

The calculated barrier heights for the forward and reverse reactions of **1c** offer an explanation for the otherwise puzzling reaction of **1d** with *N*-benzylidene-*tert*-butylamine. Sato et al. have reported that the more strained [2 + 2] product (**4d**) is formed upon prolonged heating of the [4 + 2] product (**3d**),[20k] as shown in eq 5. The lowest calculated barrier is clearly for the formation of **3c**. However, if there is sufficient energy for this to undergo the retro [4 + 2] (31.3 kcal/mol), then there is also sufficient energy to surmount the barrier to form **4c1** (23.0 kcal/mol), but there does not have to be sufficient energy to equilibrate **3c** and **4c1** (44.6 kcal/mol). The high barrier traps **4d**.

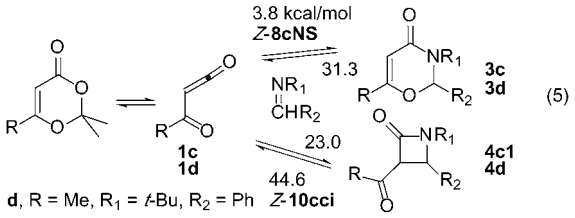

(5)

1,5-Hydrogen Shifts. One of the consequences of using formaldimine (**2**) as the model imine is that 1,5-hydrogen shifts from the endo-anti zwitterionic intermediates *Z*-**9aNA**, *Z*-**9bNA**, and *Z*-**9cNA** are possible, as shown in Scheme 1 and eq 6. Similar shifts are not likely to be as important in the case of N-substituted imines. Transition structures corresponding to these 1,5-H shifts were located and have quite low calculated barriers from the intermediates (6.0 kcal/mol, **13a**, −0.7kcal/mol, **13b**, and −1.2 kcal/mol, **13c**). It is the inclusion of the zero-point vibrational energy correction that gives these legitimate transition structures (**13b** and **13c**) their negative barriers. These transition structures are shown in Figure 6, and related energies are in Table 4.

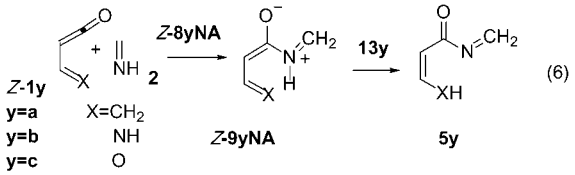

(6)

The zwitterionic intermediates (*Z*-**9aNA**, *Z*-**9bNA**, *Z*-**9cNA**) leading to the 1,5-H shifts are all planar. Transition state structures **13b** and **13c** for H-transfer in the imidoyl and formyl cases are also planar, while the transition structure **13a** for the H-shift in the vinyl case is not. The qualitative orbital interactions for these pseudopericyclic H-shifts are shown in Figure

(41) The isomeric electrocyclization transition structure based on *Z*-**11b**, but with the *E*-configuration about the C4═N5 imide bond, was not studied in this work. However, there is ample computational precedence that without the lone pair pointing towards C7, this reaction would be pericyclic, not pseudopericyclic, and would have a significantly higher barrier. See references 39a,b and (a) Rodríguez-Otero, J. *J. Org. Chem.* **1999**, *64*, 6842−6848. (b) Walker, M. J.; Hietbrink, B. N.; Thomas, B. E., IV; Nakamura, K.; Kallel, E. A.; Houk, K. N. *J. Org. Chem.* **2001**, *66*, 6669−6672.

(42) Hammond, G. S. J. *J. Am. Chem. Soc.* **1955**, *77*, 334−338.

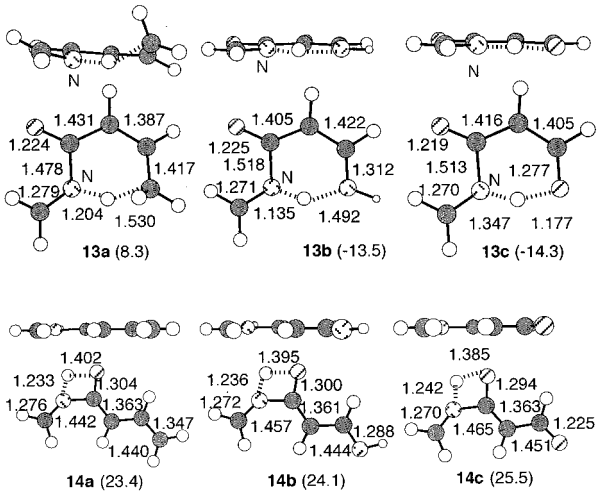

Figure 6. Side and top views of the B3LYP/6-31G* optimized transition structures for the 1,5- and 1,3-hydrogen shifts. See Figure 2 for key.

Table 4. Calculated Relative Energies (kcal/mol), Relative Energies with Zero-Point Vibrational Energy Corrections (ZPE, kcal/mol), Relative Energies from the Precursor Zwitterion (+ZPE, kcal/mol), Low or Imaginary Frequencies (cm^{-1}), and Free Energies (kcal/mol) for Structures Related to 1,5- and 1,3-Hydrogen Shift Reactions

structure	relative energy[a]	relative energy + ZPE	barrier from zwitterion	low frequencies	free energy
5a	−28.6	−25.9		65.0	−23.2
5b	−32.0	−28.9		53.5	−26.2
5c	−21.8	−18.5		73.8	−15.4
6a	−10.5	−7.9		91.9	−4.6
6b	−6.6	−4.1		92.2	−1.1
6c	−6.1	−3.8		99.0	−0.8
13a	8.4	8.3	5.0	1356.5i	12.3
13b	−14.3	−13.5	−0.9	325.4i	−9.8
13c	−14.8	−14.3	−1.5	786.9i	−10.6
14a	24.3	23.4	15.6	1673.0i	26.4
14a2	25.7	24.9	15.6	1686.7i	28.0
14b	24.9	24.1	*b*	1667.9i	26.9
14b2	30.5	29.5	*b*	1668.6i	31.6
14c	26.5	25.5	*b*	1678.5i	28.2
14c2	30.2	29.1	*b*	1682.2i	31.4

[a] All energies are relative to the lowest energy complexes, *Z*-**7aXA**, *Z*-**7bXA**, and *Z*-**7cXA**. [b] No corresponding zwitterion was located.

5C and D, and the NBO analysis is in Scheme S1. In both **13b** and **13c**, the hydrogen is transferred in the molecular plane, to a lone pair on N5 or O5. The lack of cyclic orbital overlap, combined with favorable geometries and electronic interactions, are the origin of the extremely low barriers for these hydrogen transfers.[19d] As the result of these very low barriers, formation of the zwitterionic intermediates becomes the rate-determining step. The relative energies of these transition structures, *Z*-**8bNA** and *Z*-**8cNA**, are 2.9 and 2.1 kcal/mol, respectively.

Pseudopericyclic 1,3- and 1,5-sigmatropic rearrangements have been widely observed and calculated in α,β-unsaturated ketenes.[19d,20h,31c,h,i,43] Wentrup et al. have argued that the low barriers are a consequence of favorable HOMO−LUMO interactions.[43f,g] While this is clearly important, there are such interactions in many pericyclic reactions that have more substantial barriers.[8,44] Thus, HOMO−LUMO interactions do not offer a complete explanation.

For the hydrogen transfer to occur in the vinyl case, the molecule cannot remain planar. Either the hydrogen moves out of the plane of the molecule, or the p-orbital on the CH_2 (C5) rotates into the plane, or a combination of both motions can occur, as is indeed the case. These out-of-plane motions weaken the bonding and are the origin of the larger barrier for **13a** as compared to the other two. This transition structure has a single orbital disconnection at N6, which makes it pseudopericyclic, as confirmed by the NBO analysis in Scheme S1.[19f] Thus, the barrier is lower than a hydrocarbon 1,5-hydrogen shift, but higher than **13b** and **13c**, which have two orbital disconnections and fully planar transition structures.[45]

1,3-Hydrogen Shifts. The orbital symmetry rules predict that thermal, suprafacial 1,3-shifts in hydrocarbons are forbidden.[8,46] However, 1,3-shifts become allowed with a pseudopericyclic orbital topology (Figure 5E, Scheme S1).[19d,22c] Indeed, 1,3-silyl migrations have been observed in the reactions of *N*-silylimines with ketenes.[6n] The syn zwitterions from **1a**, **1b**, and **1c** all have a hydrogen poised to transfer to the oxygen and doing so would neutralize the zwitterions (eq 7). Transition structures (*Z*- and *E*-**14a**, *Z*- and *E*-**14b**, *Z*- and *E*-**14c**) were located for 1,3-hydrogen shifts from all six of the exo-syn zwitterions (*Z*- and *E*-**9aXS**, *Z*- and *E*-**9bXS**, and *Z*- and *E*-**9cXS**, respectively). Representative structures are shown in Figure 6. The planar geometries and NBO analysis (Scheme S1) are consistent with these being pseudopericyclic reactions. The calculated barriers of 23.4, 24.1, and 25.5 kcal/mol, respectively, are low enough to be easily surmounted at room temperature. Nevertheless, they are relatively high as compared to the practically nonexistent barriers to the 1,5-hydrogen shifts. However, there is certainly angle strain in these transition structures. The hydrogen is clearly not being transferred along a linear path, nor are the angles at the nitrogen and oxygen favorable. The angle strain in these transition structures might be crudely estimated to be the strain of a cyclobutane ring, 26.5 kcal/mol.[47] This indicates again that there is a relatively low barrier for the 1,3-hydrogen shift. Thus, it would seem that both the 1,5- and 1,3-hydrogen shifts are allowed, as expected for a pseudopericyclic reaction.

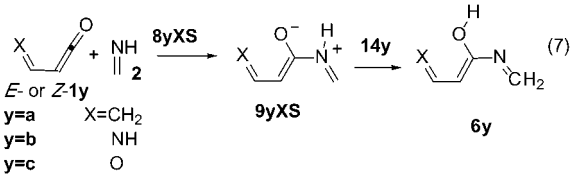

Conclusions

Although vinylketene (**1a**), imidoylketene (**1b**), and formylketene (**1c**) are all π conjugated, calculations at the B3LYP/6-

(43) (a) Wentrup, C.; Netsch, K. P. *Angew. Chem., Int. Ed. Engl.* **1984**, *23*, 802. (b) Kappe, C. O.; Kollenz, G.; Leung-Toung, R.; Wentrup, C. *J. Chem. Soc., Chem. Commun.* **1992**, 487−490. (c) Kappe, C. O.; Kollenz, G.; Netsch, K.-P.; Leung-Toung, R.; Wentrup, C. *J. Chem. Soc., Chem. Commun.* **1992**, 488−490. (d) Fulloon, B.; El-Nabi, H. A. A.; Kollenz, G.; Wentrup, C. *Tetrahedron Lett.* **1995**, *36*, 6547−6550. (e) Fulloon, B. E.; Wentrup, C. *J. Org. Chem.* **1996**, *61*, 1363−1368. (f) Koch, R.; Wong, M. W.; Wentrup, C. *J. Org. Chem.* **1996**, *61*, 6809−6813. (g) Koch, R.; Wong, M. W.; Wentrup, C. *J. Org. Chem.* **1997**, *62*, 1908.

(44) (a) Fukui, K. *Acc. Chem. Res.* **1971**, *4*, 57. (b) Bach, R. D.; Wolber, G. J.; Schlegel, H. B. *J. Am. Chem. Soc.* **1985**, *107*, 2837−2841. (c) Houk, K. H.; Gonzalez, J.; Li, Y. *Acc. Chem. Res.* **1995**, *28*, 81.

(45) (a) Jensen, F.; Houk, K. N. *J. Am. Chem. Soc.* **1987**, *109*, 3139−3140. (b) Saettel, N. J.; Wiest, O. *J. Org. Chem.* **2000**, *65*, 2331−2336.

(46) Pearson, R. G. *Symmetry Rules for Chemical Reactions*, 1st ed.; John Wiley and Sons: New York, 1976.

(47) (a) Engler, E. M.; Andose, J. D.; Schleyer, P. v. R. *J. Am. Chem. Soc.* **1973**, *95*, 8005−8025. (b) Wiberg, K. B.; Bader, R. F. W.; Lau, C. D. H. *J. Am. Chem. Soc.* **1987**, *109*, 1001−1012.

31G* level predict there to be significant differences when they react with formaldimine (**2**), both in their preference for [4 + 2] versus [2 + 2] pathways as well as their preference for stepwise versus concerted mechanisms. It is now possible to provide answers to the questions posed in the Introduction: What factors influence the periselectivity for [2 + 2] versus [4 + 2] cycloadditions? Are pseudopericyclic orbital topologies important? Why are the mechanisms of the [2 + 2] cycloadditions of ketene with imines and alkenes different?

For all three ketenes (**1a**, **1b**, and **1c**), concerted [4 + 2] cycloaddition pathways with **2** could be found. The transition structure for vinylketene (*Z*-**12a**, 17.6 kcal/mol) is nonplanar and pericyclic, while those for imidoylketene (***Z*-12b**, 9.2 kcal/mol) and formylketene (***Z*-12c**, 6.6 kcal/mol) are more nearly planar, have significantly lower barriers, and can be understood as pseudopericyclic.

Stepwise [4 + 2] pathways were found for **1b** and **1c** (but not for **1a**) reacting with **2** and are calculated to be the lowest energy pathways for these ketenes. The rate-determining steps are the formation of the zwitterionic intermediates, while the electrocyclic ring closures have extremely low barriers (*Z*-**11b**, 1.1 kcal/mol from *Z*-**9bNS** and *Z*-**11c**, 0.7 kcal/mol from *Z*-**9cNS**) and are essentially planar at N5 or O5. Thus, these reactions are also pseudopericyclic. The low barrier for the pseudopericyclic [4 + 2] cycloaddition and retrocycloaddition of **1c** and **2** provides an explanation of the thermal equilibration from a six-membered adduct (**3d**) to a four-membered adduct (**4d**), observed by Sato et al. (eq 5).

Both stepwise and concerted pathways for [2 + 2] cycloadditions are calculated for all three ketenes, **1a**, **1b**, and **1c**. The concerted transition structures (*Z*- and *E*-**10x**π**y**, **x** = **a**, **b**, **c**; **y** = **i**, **o**) are closely related to the transition structure for the cycloaddition of ketene with ethylene, both in terms of geometries (see Figure S11) and barriers (28.3−35.6 kcal/mol). In these transition structures, the π-system of the imine, but not the nitrogen lone pair, participates in bond formation. The most consistent interpretation of these transition states is that proposed by Yamabe et al.,[11] that the orthogonal orbitals of the ketene remove the orbital symmetry constraints, in other words, that the concerted [2 + 2] cycloadditions of ketene with π-bonds are pseudopericyclic.

In the stepwise mechanism, nucleophilic attack of the imine lone pair on the ketene in-plane LUMO generally leads to the zwitterionic intermediates, although in some cases steric crowding precludes a stable intermediate. The zwitterions lie in shallow minima, and there is facile equilibration between them; the rate-determining step is the pericyclic, conrotatory electrocyclic ring closure. These transition structures manifest torquoselectivity as well; vinyl and imidoyl substituents rotate outward, but the formyl substitutent prefers inward rotation, in agreement with Houk's original work. The barriers for these electrocyclizations increase from 16.9 kcal/mol (*E*-**10aco**) to 20.2 kcal/mol (*E*-**10bco**) and 23.3 kcal/mol (*E*-**10cci**). This trend reflects the stabilization of ketene by electron-withdrawing substituents.

There has been ongoing controversy regarding the mechanism of the [2 + 2] cycloaddition of ketenes with imines. The existence of two pathways, stepwise and concerted, provides a resolution of this confusion. Previous workers had, in general, calculated one or the other, but none had recognized that the concerted reaction is analogous to the cycloaddition of ketene with an alkene. The stepwise pathway is followed with imines, not because of any destabilization of the concerted reaction, but simply because of the lower barriers for electrocyclization of the zwitterions.

To summarize, for vinylketene (**1a**), the stepwise [2 + 2] and concerted [4 + 2] pericyclic cycloadditions have similar barriers, with the [2 + 2] generally lower in energy. The rate-determining steps in both pathways are pericyclic, an electrocyclization and a cycloaddition, respectively. The [4 + 2] cycloaddition is predicted to be competitive if **1a** is constrained to the *Z*-conformation. For imidoylketene (**1b**) and formylketene (**1c**), both the stepwise and concerted [2 + 2] cycloadditions are also pericyclic and have comparable energies to **1a**, but both the stepwise and concerted [4 + 2] cycloadditions have dramatically lower barriers, with the stepwise reactions favored. The low barriers are a direct consequence of the availability of in-plane lone pairs in **1b** and **1c** for the pseudopericyclic orbital topology in the [4 + 2] cycloadditions.

The choice of formaldimine (**2**) as the model imine led to calculation of both 1,3- and 1,5-hydrogen shifts. These are calculated from the *Z*- and *E*-**9yXS** (exo, syn) and from the *Z*-**9yNA** (endo, anti) zwitterions, respectively. Although 1,3- and 1,5-shifts are not generally significant in reactions of substituted imines, 1,3-shifts are observed in *N*-silylimines. Both the 1,3- and 1,5-hydrogen shifts have low barriers and planar transition structures; these reactions are also best interpreted as pseudopericyclic.

The barrier heights and changes in favored pathways in these reactions can be understood by considering the pseudopericyclic orbital topology of **1b** and **1c**. The three defining characteristics of pseudopericyclic reactions are all illustrated in comparisons among the plethora of pericyclic and pseudopericyclic reactions reported herein. Specifically, low or nonexistent barriers, planar transition structure geometries, and cyclic reactions that are allowed irrespective of the number of atoms are calculated for pseudopericyclic [4 + 2] cycloadditions and 1,3- and 1,5-hydrogen shifts of **1b** and **1c**. In contrast, higher barriers and nonplanar transition structures are found for the pericyclic reactions.

Acknowledgment. We thank the Robert A. Welch Foundation for support of this work and the Texas Tech University High Performance Computing Center for computer time.

Supporting Information Available: Figures of all optimized structures (12 figures); one table detailing constrained attempted optimizations; absolute energies, zero-point energies, low or imaginary frequencies for all optimized structures (five tables); summary of NBO analysis (one scheme) (PDF). This material is available free of charge via the Internet at http://pubs.acs.org.

JA017559Z